JACS
JOURNAL OF THE AMERICAN CHEMICAL SOCIETY
Article
pubs.acs.org/JACS

Photoswitchable Nanoparticles for Triggered Tissue Penetration and Drug Delivery

Rong Tong,[†,‡] Houman D. Hemmati,[‡] Robert Langer,[†] and Daniel S. Kohane*[,‡]

[†]Department of Chemical Engineering, Massachusetts Institute of Technology, 77 Massachusetts Avenue, Cambridge, Massachusetts 02139, United States

[‡]Laboratory for Biomaterials and Drug Delivery, Department of Anesthesiology, Division of Critical Care Medicine, Children's Hospital Boston, Harvard Medical School, 300 Longwood Avenue, Boston, Massachusetts 02115, United States

Supporting Information

ABSTRACT: We report a novel nanoparticulate drug delivery system that undergoes reversible volume change from 150 to 40 nm upon phototriggering with UV light. The volume change of these monodisperse nanoparticles comprising spiropyran, which undergoes reversible photoisomerization, and PEGylated lipid enables repetitive dosing from a single administration and enhances tissue penetration. The photoswitching allows particles to fluoresce and release drugs inside cells when illuminated with UV light. The mechanism of the light-induced size switching and triggered-release is studied. These particles provide spatiotemporal control of drug release and enhanced tissue penetration, useful properties in many disease states including cancer.

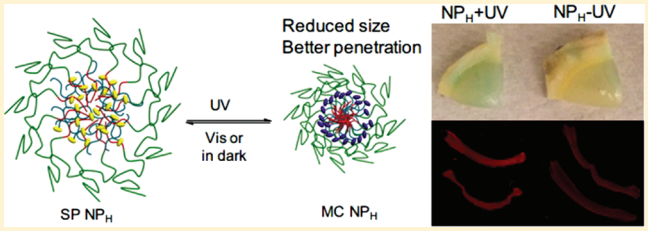

INTRODUCTION

Controlled release technology is expected to have a profound impact in many medical fields including oncology.[1] The incorporation of chemotherapeutic agents in nanoparticle (NP) delivery vehicles has improved drug solubility, reduced clearance, reduced drug resistance, and enhanced therapeutic effectiveness.[2] With controlled release NP systems, a single dose can sustain drug levels within the desired therapeutic range for long periods in various diseases (e.g., diabetes[3] or cancer[4]). Several nanoparticulate therapeutics, for example, Doxil (~100 nm PEGylated liposome loaded with doxorubicin) and Abraxane (~130 nm albumin-bound paclitaxel nanoparticles), have been approved by the FDA, and have shown improved pharmacokinetics and reduced adverse effects compared to their parent drugs.[5] However, currently approved nanomedicines provide modest survival benefits for patients,[5,6] perhaps in part because of poor tumor penetration.

Nanoparticle size is one crucial determinant of accumulation and penetration into tumor tissue.[7] Nanoparticles with sub-100 nm sizes are optimal for the enhanced permeation and retention (EPR) effect for passive tumor targeting.[8] However, physiological barriers, such as the dense interstitial matrix—a complex assembly of collagen, glycosaminoglycans, and proteoglycans—hinder the delivery of drugs throughout the entire tumor.[9] For example, Doxil (~100 nm) is found trapped near the tumor vasculature.[10] Although the small size (molecular weight = 544 Da) of doxorubicin released from Doxil allows rapid diffusion, doxorubicin cannot migrate far from the particles due to rapid uptake of doxorubicin by perivascular cells, which results in heterogeneous therapeutic effects.[11] Deep penetration of nanoparticles in tumors is necessary to enhance their therapeutic effect.[12]

Another significant drawback of commercially available drug delivery NPs is that drugs are released at a predetermined rate irrespective of patient needs or changing physiological circumstances. A triggerable drug delivery system would allow repeated on-demand dosing that would be adaptable to the patients' regimen and allow multiple dosages from a single administration.[13] It might also help address the potential importance of timing on therapeutic effect ("chrono-administration") in the treatment of cancer,[14] a concept that is receiving burgeoning recognition, for example, the periodicity of VEGF expression in breast cancer regulates tumor cancer vascular permeability.[15] Another clinical example of the importance of timing is that periodic infusion of angiotensin II via the tail vein can enhance macromolecular delivery into tumors by overcoming the barrier of elevated interstitial fluid pressure within tumors; no such increase of macromolecular uptake occurs either by an acute or chronic increase in blood pressure induced by angiotensin II.[16] Furthermore, the permeability of many tumor models varies with time and in response to treatment, so that vascular pore sizes vary greatly, resulting in heterogeneous NP extravasation and drug delivery efficacy.[5,17] On-demand drug release from NPs accumulated in tumors could allow in situ chrono-administration, potentially increasing drug retention in cancers, maximizing tumor killing and minimizing metastatic spread.

Received: December 20, 2011
Published: March 5, 2012

   dx.doi.org/10.1021/ja211888a | J. Am. Chem. Soc. 2012, 134, 8848−8855

Here, we have developed a photoswitching nanoparticulate system that uses light as the remote means of triggering both on-demand drug release and reversible changes in particle volume to enhance tissue penetration.

RESULTS AND DISCUSSION

Photochromic properties are controllable light-induced changes in color or reversible photoexcited transformations between two isomers.[18] There has been intensive investigation of photochromic materials for applications from sunglasses to optically rewritable data storage,[19] optical switching,[20] and chemical sensing.[21] The photoswitchable NPs developed here were composed of spiropyran (SP, a family of photochromic molecules, Figure 1a,b) and lipids. SP consists of a nitro-

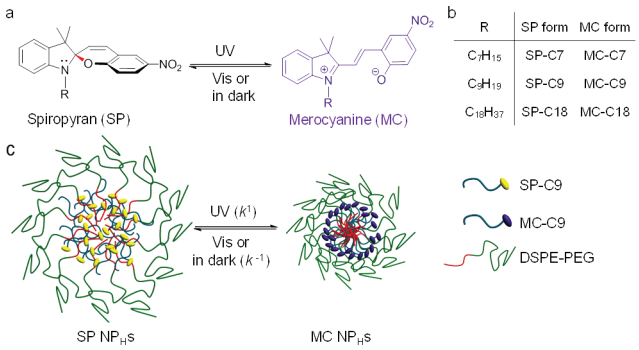

Figure 1. (a) Structure and photoisomerization reaction between spiropyran (SP) and merocyanine (MC). (b) Abbreviations for SP and MC derivatives. (c) Scheme of photoswitching SP NP_Hs composed of SP-C9 and DSPE-PEG. Yellow oval, SP molecule; blue line, the alkyl chain (R) in SP; red, lipid part; green line, PEG. SP NP_Hs are converted to MC NP_Hs (purple sphere: MC molecule) by UV light irradiation; the reversible photoisomerization from MC NP_Hs to SP NP_Hs happens in dark but is accelerated by visible light (500−600 nm).

benzopyran and an indoline moiety with orthogonal orientation (Figure 1a). Both moieties absorb in the ultraviolet spectrum independently.[22] Ultraviolet light (UV, 365 nm) induces ring-opening in the pyran to form merocyanine (MC, Figure 1a). The nitrophenol and indoline chromophores are merged to form one large planar π-system, leading to intense absorption in the visible (Vis) spectral region (500−600 nm).[23] The zwitterionic MC form is less stable than the hydrophobic SP form and undergoes spontaneous ring-closing back to SP in the dark that is accelerated by photoexcitation of MC in the Vis absorption band.[18a] The polarity or hydrophilicity changes of SP molecules that accompany their photoisomerization have been suggested to alter microenvironments within polymers and supermolecular assemblies such as Langmuir−Blodgett films, micelles, and liposomes.[20b,24] We hypothesize that SP isomerization upon irradiation would lead to hydrophilicity changes which would switch the NPs' physical assembly properties and trigger drug release. Of note, micromolar concentrations of SP derivatives are reported to have minimal cytotoxicity in macrophages, gastric cells, and epithelial cells after exposure for 72 h.[25] These properties suggest that SP is a suitable base material for light-responsive NPs for triggered release.

Formulation of Photoswitchable NPs with Light-Triggered Size Changes. SP derivatives bearing hydrophobic alkyl chains (Figure 1a,b) were synthesized by coupling 2-hydroxy-5-nitrobenzaldehyde with substituted 2,3,3-trimethyl-3*H*-indolium iodide (Figure S1a). NPs were initially prepared by direct nanoprecipitation of SP alone (an extensively used simple method for the preparation of NPs with therapeutic agents embedded in the hydrophobic matrices).[26] An acetonitrile solution of SP-C9 (10 mg/mL) was nanoprecipitated into water (final acetonitrile/water = 1/40, v/v), resulting in NP sizes of 198.1 ± 2.5 nm with a polydispersity of 0.09 ± 0.02, determined by dynamic light scattering (DLS, N = 5, Table S1).

Irradiation of the SP-C9 NPs with UV light (365 nm, intensity ∼1 W/cm^2, ∼ 3.1 × 10^{-6} einstein) led to photoisomerization and the subsequent conversion of hydrophobic SP-C9 to amphiphilic MC-C9, and a change in the sizes of the NPs. The irradiated NPs had a bimodal size distribution (Figure S1b), with one peak at 39.6 ± 3.0 nm (N = 5, 99.1% of number population, determined by DLS; attributable to NPs assembled by MC-C9), and another at 202.1 nm (0.9% of number population; attributable to NPs formed with SP-C9). After irradiation, the colorless NP solution became purple, with a strong Vis absorption band characteristic of MC-C9 (maximum absorption wavelength λ_{max} = 560 nm; Figure S1c,d). Nanoprecipitation of a SP analogue with a shorter alkyl chain, SP-C7, produced NPs that did not undergo a significant size change upon UV irradiation (Table S1).

SP-C9 NPs formed in aqueous solution aggregated when introduced into PBS (Table S1), presumably due to salt-induced screening of electrostatic repulsive forces between particles.[27] In addition, the NPs had low actual drug loadings wt % (loading wt % < 1%) and efficiencies (<13%; Table S2). The loading efficiency did not increase in NPs made of SPs with a longer alkyl chain (SP-C18, Table S2). Higher drug loading of delivery vehicles is desirable for optimal therapeutic effect, to enhance the potency of NPs that reach the tumors.[28]

To improve the stability and loading efficiencies of NPs while maintaining the NPs' photoswitching properties, we produced hybrid SP/lipid-polyethylene glycol (PEG) NPs (termed NP_Hs; Figure 1c) using a rapid ultrasonication method.[29] An acetonitrile solution of SP-C9 (1 mg/mL) was slowly added into a 4 wt % ethanolic aqueous solution containing lecithin and 1, 2-distearoyl-*sn*-glycero-3-phosphoethanolamine-*N*-carboxy(polyethylene glycol)-5000 (DSPE-PEG, [SP-C9]/[DSPE-PEG]/[lecithin] = 32/16/1), followed by addition of water to adjust the organic/aqueous solution volume ratio to 1/10. After sonication for 8 min and filtration of the organic solvent, SP NP_Hs were obtained with an average hydrodynamic diameter of 143.2 ± 2.1 nm and a polydispersity of 0.03 ± 0.01 (N = 5, Figure 2a). SP-C9 was not detected by HPLC in the filtrate after repetitive washing of the NP_Hs by ultracentrifugation, indicating that SP-C9 was completely incorporated into NPs (Figure S2a,b). After UV illumination (30s, ∼100% conversion to MC), the absorption band of the NP_Hs moved to a λ_{max} at 551 nm (Figure 2b). As with the nonhybrid NPs, UV irradiation of NP_Hs induced a size change (to 47.1 ± 1.3 nm, polydispersity of 0.05 ± 0.02, N = 5). These results confirmed that both the photochromic properties of SP-C9 and light-triggered size change were maintained in the SP NP_Hs.

MC NP_H reverted to SP NP_H in darkness or by Vis light, with an accompanying increase in volume (Figure 2a). Consequently, there could be inaccuracies in measuring MC NP_H size by relatively slow techniques such as DLS. To confirm particle shrinkage after irradiation (Figure 2a), we produced NP_H containing MC−CN, a similar but relatively stable MC

dx.doi.org/10.1021/ja211888a | J. Am. Chem. Soc. 2012, 134, 8848−8855

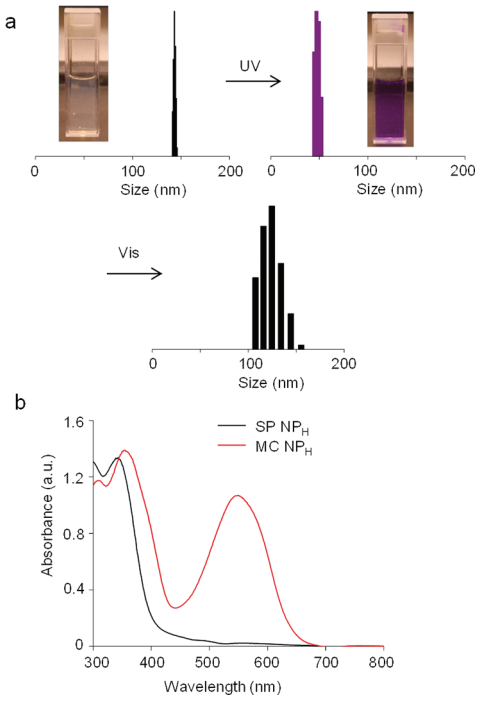

Figure 2. (a) Dynamic light scattering measurement of size changes of SP-C9/DSPE-PEG/lecithin SP NP$_H$s upon alternating UV (30 s) and visible light (3 min) illumination. Inset: the solution of NP$_H$ before and after UV irradiation. (b) Steady-state absorption spectra of NP$_H$ ([SP-C9] = 0.46 mM) and their corresponding isomerized MC NP$_H$ (λ_{max} = 551 nm) upon UV light irradiation.

quinoidal structure, which is a 1, 6-addition adduct of MC-C9 with trimethylsilyl cyanide (Figure S3).[30] MC−CN NP$_H$s were 59.4 nm in diameter, with a polydispersity of 0.04 (Figure S3c), similar to the size of MC NP$_H$ produced from SP NP$_H$ by UV-irradiation (47.2 nm with a polydispersity of 0.05, Figure 2a). Direct nanoprecipitation of MC−CN resulted in 42.6 nm NP$_H$s with a polydispersity of 0.11 (Figure S3d), a result consistent with the DLS measurements of MC NP$_H$s.

The PEGylated lipid was designed to give NP$_H$s a relatively neutral surface charge for prolonged circulation and stabilization.[31] The ζ potential of SP NP$_H$ and MC NP$_H$ at pH 7.5 was −6.25 ± 0.31 mV and −5.12 ± 0.12 mV, respectively. The results indicated the similarly neutral charges of NP$_H$ before and after irradiation. No aggregation was observed for over 4 h in PBS (Figure S2c). The stability of NP$_H$s was also evaluated in serum by monitoring the absorbance change at 560 nm, since nanoparticles cannot be accurately detected in dense serum solutions by DLS.[32] No significant aggregation was observed over 4 h.

For eventual clinical translation, it has to be possible for NPs to be stable during manufacturing, storage, and transportation.[33] SP NP$_H$s were lyophilized for 48 h with bovine serum albumin (BSA, NP/BSA = 1/15, w/w), a known lyoprotectant reagent,[34] then stored at −20 °C for over one month. The subsequent reconstitution of lyophilized SP NP$_H$ in PBS did not significantly change the NP$_H$ sizes and photochromic properties (Figure S4). Lyophilization of SP NP$_H$ in water (without albumin) led to micrometer-sized, nondispersible aggregates upon reconstitution in PBS. Since albumin is used clinically, this lyoprotection strategy may be useful for potential translational of SP NPs.

To examine whether this formulation could be used to form NPs containing a broad range of compounds, we tested the ability to encapsulate rhodamine B, coumarin 6, cyanine 5 (Cy5), paclitaxel, docetaxel, proparacaine, and doxorubicin. NPs with adjustable loadings up to 10 wt % (with relatively high loading efficiencies) and low polydispersities were readily obtained for all of the therapeutics (docetaxel, doxorubicin, proparacaine) and dyes (Cy5, rhodamine B, coumarin 6) tested (Table 1).

HeLa (cervical cancer cell), PC-3 (human prostate carcinoma), and human umbilical vein endothelial cells (HUVEC) were used to assess the cytotoxicity of SP NP$_H$s. Following 72 h of exposure to NPs, cell viability was determined by the MTT (3-(4,5-dimethylthiazol-2-yl)-2,5-diphenyltetrazolium bromide) assay.[35] The SP NP$_H$ did not cause significant cytotoxicity in either cell line except at extremely high concentrations (Figure S5a). The EC_{50} values (the concentrations at which cell viability was reduced by 50%, determined by interpolation from the data in Figure S5a) for the [SP-C9] in those NP$_H$s were 9.53 mM for HUVEC (6.33 mg/mL NP$_H$s), 7.01 mM for HeLa cells (4.66 mg/mL NP$_H$s), and 7.41 mM for PC-3 cells (4.92 mg/mL NP$_H$s). In a 70 kg adult, these EC_{50} values are approximately equivalent to 70 g/dose (~ 1 g/kg) assuming NP$_H$s are restricted to the 14 L extracellular fluid, or 25 g/dose (~350 mg/kg) if the NPs are restricted to the 5 L bloodstream, extremely high doses compared to those used clinically with Doxil (dosage: 50 mg/

Table 1. Characteristics of Photoswitching SP NP$_H$[a]

drug/dye	initial LD %	actual LD %	LD efficiency %	size (nm)	polydispersity	size-UV (nm)	polydispersity
Rhodamine B	5	2.49 ± 0.13	49.8	129.7 ± 1.8	0.054	74.2 ± 2.6	0.081
Coumarin 6	10	6.84 ± 0.07	68.4	74.7 ± 2.9	0.013	27.2 ± 4.5	0.086
Calcein	5	2.71 ± 0.09	54.2	133.9 ± 6.7	0.064	50.6 ± 4.8	0.072
Cyanine 5	10	9.41 ± 0.05	94.1	108.6 ± 4.5	0.071	72.7 ± 0.8	0.066
Paclitaxel	5	3.97 ± 0.04	79.4	101.7 ± 3.1	0.052	40.1 ± 8.9	0.065
Paclitaxel	10	8.21 ± 0.14	82.1	116.1 ± 1.1	0.088	76.1 ± 5.2	0.066
Docetaxel	10	7.42 ± 0.11	74.2	125.4 ± 5.0	0.039	49.7 ± 5.8	0.043
Doxorubicin	5	2.69 ± 0.21	53.7	96.9 ± 4.7	0.035	41.5 ± 6.4	0.043
Doxorubicin	10	4.96 ± 0.14	49.6	93.3 ± 3.2	0.074	49.8 ± 6.7	0.058
Proparacaine	10	6.35 ± 0.16	63.5	87.5 ± 2.7	0.049	48.2 ± 5.4	0.100
Proparacaine	15	7.64 ± 0.19	51.0	102.3 ± 6.6	0.071	66.1 ± 2.5	0.032

[a]Determined by DLS and HPLC. Abbreviations: LD, loading; size-UV, sizes of NPs treated by UV irradiation (N = 5). Data are means ± SD (N = 5).

dx.doi.org/10.1021/ja211888a | J. Am. Chem. Soc. 2012, 134, 8848−8855

m^2).[36] The EC_{50} value for MC NP_H in HeLa cells was 3.46 mg/mL, similar to that for SP NP_H (Figure S5b).

Repetitive Photoswitching and Light-Triggered Drug Release Profiles of NPs. The repeatability of the photoswitching property of NP_H was evaluated by alternating cycles of UV and Vis light. This modulation was fully reversible for at least 4 continuous cycles (UV irradiation for 30 s and Vis light for 3 min, Figure 3). However, the absorbance at the MC-C9

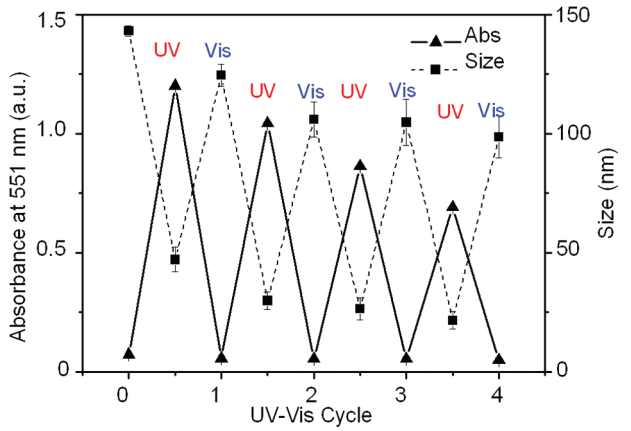

Figure 3. Reversible NP_H photochromism (solid line, Abs: absorbance) and size switching (dashed line) with alternating UV ("UV", 30 s) and visible light ("Vis", 3 min) irradiation. The modulation of NP_H size and photochromism was fully reversible for at least 4 cycles. Data are means ± SD, N = 4.

peak maximum decreased 43% after 4 cycles, and was accompanied by a reduction in size from 143.2 to 98.7 nm in the SP state (Figure 3). The decrease of absorbance after repetitive irradiation could be due to photofatigue (the loss of performance in photoisomerization) — a common property of organic photochromic compounds.[37] The absorption intensity of MC in NP_H at 551 nm faded at a rate dependent on the UV (365 nm) irradiation time, and that antioxidant agents could not eliminate the decrease in MC-C9 absorption, suggesting an O_2-independent fatigue mechanism for photofatigue in SP NP_Hs (see Figure S6 and Scheme S1 and associated discussion).

We hypothesized that the phototriggered shrinkage of NP_Hs might induce drug release. In the absence of UV phototriggering, drugs (e.g., doxorubicin) and dyes (e.g., rhodamine 6B) loaded in SP NP_H showed slow release in PBS that was complete within 48−72 h (Figure 4, Figure S7). Upon UV irradiation (30s), NP_Hs encapsulating rhodamine 6B (loading wt% = 4.3%) released 29.3% of the loaded dye within 1 h as determined by HPLC, while 7.2% was released in the same period without UV irradiation. Of note, the release kinetics of NP_Hs that had been triggered (Figure 4, blue line) eventually slowed to a rate similar to that of NP_Hs that were not irradiated (Figure 4, black line). This decrease in the release rate could be explained by the majority of the MC-C9 in NPs spontaneously converting back to SP-C9, resulting in NPs reassembled in their original structure. In a separate group, UV triggering (30 s irradiation) was conducted every 3 h for three cycles (Figure 4, green line), with an increase in release at each event.

UV-triggered release was demonstrated in cells by fluorescence imaging of SP NP_H loaded with calcein. Calcein was selected because its fluorescence self-quenches while it is entrapped inside particles, whereas calcein released from

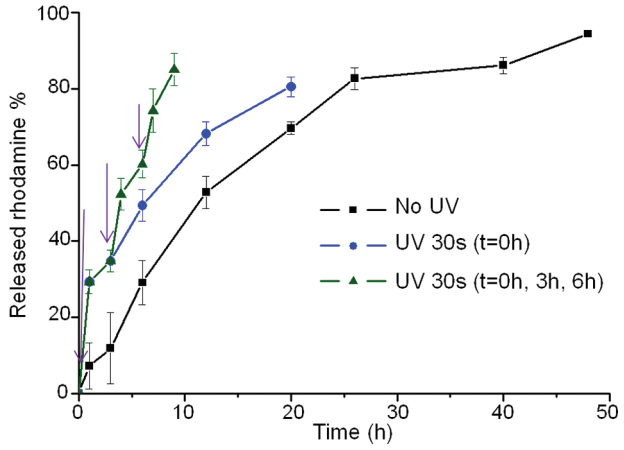

Figure 4. Release profiles in PBS for rhodamine B loaded in SP NP_H under different conditions: without irradation; with UV irradiation for 30 s at 0 h; with repetitive UV irradiation at 0, 3,and 6 h. The times of irradiation are indicated by purple arrows. Data are means ± SD, N = 6.

particles will become diluted and fluoresces.[38] SP NP_H loaded with calcein (2.7 wt %) were incubated with HeLa cells. After 4 h, the media containing NP_Hs was removed and the cells were washed with PBS. Cells in medium were then illuminated by UV (365 nm) for 2 s, left in darkness for 5 min, then imaged (Figure S8). Strong fluorescence intensity with an emission maximum at 510 nm was noted in the cells, indicating that the calcein was released from NPs that had been taken up. Illumination followed by imaging was repeated 5 times, during which the fluorescence intensity gradually increased to saturation (Figure S8a,b). Cells treated with same NPs but without UV irradiation did not fluoresce, suggesting that the UV triggered rapid calcein release and intracellular dispersal from SP NP_H. These results were validated by flow cytometry, which showed a 24.7-fold increase in fluorescence intensity after a 10 s UV treatment (Figure S8c).

Surface Functionalization of NPs. Nanoparticle therapeutic effect can be enhanced and toxicity reduced by surface modification with moieties that allow intracellular penetration and/or targeting of specific tissues.[39] To examine the potential suitability of the NP_H for targeted drug delivery, we formulated NPs (NP_M) composed of SP-C9 and a mixture of DSPE-PEG_{3400}-maleimido (DSPE-PEG-MAL) and DSPE-PEG in a 4/1 ratio (w/w), 153.1 nm in diameter and with a polydispersity of 0.09. A cell penetration peptide (Cpp) Cys-Tat (47−57) (sequence: CYGRKKRRQRRR-NH_2) was introduced onto SP NP_M loaded with Cy5 by reaction of the carboxyl-terminal Cys of the peptide with the MAL on the NP_M surface (NPs/Cpp = 100/1, w/w). The fluorescence intensity of HeLa cells incubated with the resulting NPs (SP NP_M-Cpp) for 30 min, measured by flow cytometry, was 7.1 times higher than that of cells treated with SP NP_M lacking Cpp (N = 4, fluorescence intensities of 1940 ± 215 and 273 ± 197, respectively; Figure 5a).

We compared the cytotoxicity of doxorubicin-loaded SP NP_M-Cpp (doxorubicin/SP NP_M-Cpp) to that of SP NP_M without Cpp (doxorubicin/SP NP_M). HeLa cells were incubated with doxorubicin/SP NP_M-Cpp or doxorubicin/SP NP_M for 2 h, then incubated in medium without NPs for a total of 48 h; cell viability was measured by MTT assay. The doxorubicin/SP NP_M-Cpp were significantly more cytotoxic

dx.doi.org/10.1021/ja211888a | J. Am. Chem. Soc. 2012, 134, 8848−8855

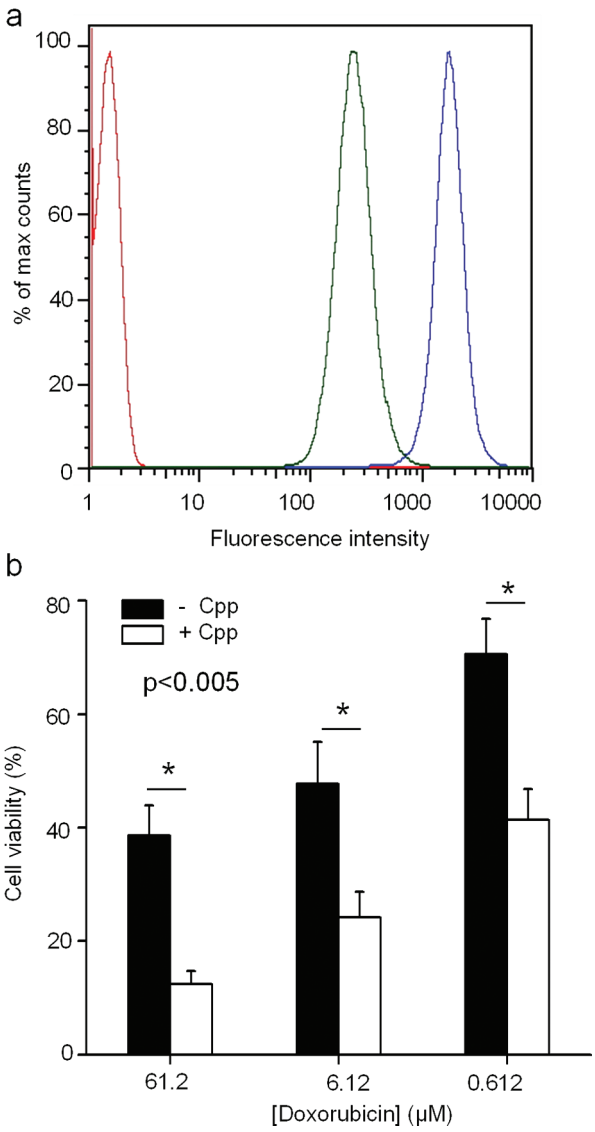

Figure 5. (a) Flow cytometric analysis of the internalization of Cy5 in SP NP_M-Cpp. Red line, untreated HeLa cells; green line, HeLa cells treated with Cy5/SP NP_M for 30 min; blue line, HeLa cells treated with Cy5/SP NP_M-Cpp for 30 min; (b) MTT assay to determine the differential cytotoxicity of doxorubicin/SP NP_M, and doxorubicin/SP NP_M. Data are means ± SD, $N = 6$, asterisks indicate $P < 0.005$.

than the doxorubicin/SP NP_M (Figure 5b). These results suggest that the SP NP_M's have the capacity to be functionalized by a broad range of biomolecules (e.g., aptamers[40] or other peptides[41]) to enhance drug delivery.

Light-Triggering Enhances Diffusion in Collagen Matrices. As discussed above, the ability to penetrate tissue could have a bearing on therapeutic effectiveness. We evaluated whether the light- triggered size change could enhance diffusive transport through a dense collagen gel at a concentration (0.74%; 7.4 mg/mL[12]) similar to the 9.0 ± 2.5 mg/mL of interstitial matrix estimated for interstitial collagen in human tumors (e.g., LS174T) and murine tumors (e.g., MCaIV).[10b,42] SP NP_Hs (1 mg/mL) loaded with 5 wt % indocyanine green (ICG), a NIR dye, were placed in contact with collagen gels in a horizontal capillary tube, then incubated for a further 12 h at 37 °C. A NIR imaging system was used to track particle infiltration into the collagen (Figure 6). Free ICG penetrated

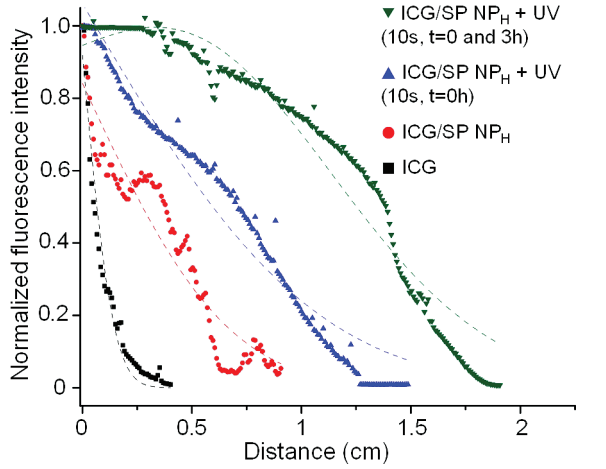

Figure 6. Normalized NIR fluorescence intensity vs distance profiles for various formulations' penetration into collagen gels over a period of 12 h (7.4 mg/mL): free ICG (black, diffusion coefficient = 3.59 ± 1.94 × 10^{-7} $cm^2 \cdot s^{-1}$), ICG/SP NP_H (red, diffusion coefficient = 7.65 ± 1.63 × 10^{-7} $cm^2 \cdot s^{-1}$), ICG/SP NP_H irradiated by UV light (blue, diffusion coefficient = 2.24 ± 0.42 × 10^{-6} $cm^2 \cdot s^{-1}$ at $t = 0$ for 10 s), and ICG/SP NP_H irradiated twice by UV (green, for 10 s each time, separated by 3 h,). Diffusion coefficient data are means ± SD, $N = 4$. The dashed lines are theoretical curves fitting the intensity profiles using a one-dimension diffusion model.

4.0 ± 0.21 mm into the collagen gels, ICG/SP NP_H penetrated 8.3 ± 0.10 mm without UV triggering, and ICG/SP NP_H triggered by UV for 10 s penetrated 12.1 ± 0.02 mm ($N = 4$, $P < 0.005$ for irradiated ICG/SP NP_H compared to free ICG and unirradiated ICG/SP NP_H). (The mechanical properties of collagen barely change after 1 h irradiation at 254 nm UV light, ~1.7 × 10^{-6} einstein.[43]) By fitting the fluorescence intensity of ICG/SP NP_H to a one-dimensional diffusion model, we obtained an average diffusion coefficient of 2.24 ± 0.42 × 10^{-6} $cm^2 \cdot s^{-1}$ for UV-triggered ICG/SP NP_H NPs ($N = 4$, $P < 0.005$ compared to free ICG), while the diffusion coefficient for unirradiated ICG/SP NP_H (7.65 ± 1.63 × 10^{-7} $cm^2 \cdot s^{-1}$, $N = 4$) was not statistically significantly different from that of free ICG (3.59 ± 1.94 × 10^{-7} $cm^2 \cdot s^{-1}$, $N = 4$, $P = 0.064$) compared to unirradiated ICG/SP NP_H (Figure 6). The relatively low diffusion rate of free ICG in collagen gels compared to NP_Hs might be partly due to the lipophilicity of ICG.[44] Gel penetration was further enhanced by increasing irradiation: ICG/SP NP_H irradiated twice (for 10 s each, separated by 3 h) penetrated 16.8 ± 0.10 mm with an average diffusion coefficient of 1.97 ± 0.28 × 10^{-6} $cm^2 \cdot s^{-1}$ (calculated by modified one dimension diffusion models; $N = 4$; Figure 6 green line). The fact that the diffusion coefficient of light-triggered ICG/SP NP_H was significantly larger than those for nonirradiated ICG/SP NP_H and free ICG (for both $P < 0.005$) suggests that light-induced shrinkage might help deepen tissue penetration of SP NP_H and their payloads. That possibility is supported by the observation that irradiation does not appear to affect the other physicochemical properties of PEGylated NP_H (they have similar slightly negatively charged surfaces before and after irradiation).

Enhanced Diffusion of Photoswitching NPs in the Cornea. We assessed the potential for photoswitching SP NP_H to carry drugs across the cornea in a manner analogous to the findings in collagen gels. Corneas are composed of 90−95 wt % of dense collagens, rendering the delivery of drugs through the

dx.doi.org/10.1021/ja211888a | J. Am. Chem. Soc. 2012, 134, 8848−8855

cornea to the anterior chamber difficult. Particles containing Cy5 (Cy5/SP NP_H) were applied to fresh cadaveric porcine corneas with or without UV light triggering for 1 min, and incubated for 8 h. Gross examination of the corneas and NIR scanning of Cy5 in corneal cross section demonstrated that the diffusion of Cy5/SP NP_H was markedly enhanced by UV light triggering (Figure 7). Histologically, corneas treated with Cy5/SP NP_H and UV light were indistinguishable from untreated controls under light microscopy, showing no tissue injury (Figure S9). Since collagen is one of the major components of the interstitial matrix, these results suggest the potential usefulness of SP NP_H for light-triggered drug delivery to targeted tissues, for example, eyes and tumors. These results are consistent with a recent report that polymeric micelles ~30 nm (close to MC NP_Hs sizes) showed enhanced tissue penetration and potent antitumor activity in poorly permeable pancreatic tumors.[45] The histological findings, together with the benign cytotoxicity (Figure S5) are consistent with a favorable safety profile, but this remains to be validated by in vivo studies.

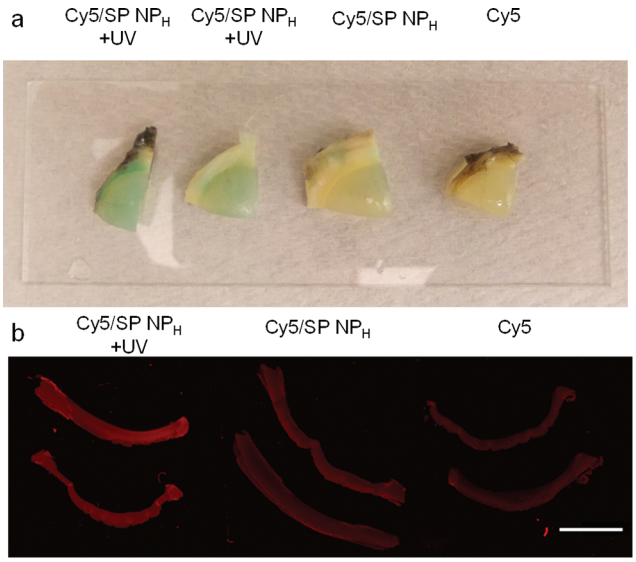

Figure 7. Ex vivo study of Cy5/SP NP_H penetration in porcine corneas. (a) Fresh corneas after an 8-h treatment with Cy5/SP NP_H (with or without UV irradiation for 1 min) or Cy5. The green color indicates the presence of Cy5 (a blue dye that becomes greenish in the slightly yellow tissue of the eye); (b) near-infrared images of cross sections of corneas tissues treated as in panel (a). The scale bar = 1 cm.

The wavelengths of the UV light we used for SP NP_H triggering might limit the application of this technology to areas of the body that can be illuminated directly, for example, the eyes and ears. Of note, the photochromic conversion of SP could be potentially triggered at depths up to several centimeters by near-infrared lasers using two-photon technology (wavelength ~ 720 nm), through soft tissues, bone, and intact skull.[46]

Fluorescence of Photoswitching NPs. The possibility that NP_H could perform as fluorescent light-triggered imaging probes was suggested by the fact that SP or nanoparticles surface-modified with SP have been utilized as fluorescence imaging probes in different microscopy techniques, including optical lock-in detection (OLID),[27] two-photon photoswitching, and imaging by noninvasive near-infrared (NIR) light.[28]

Although MC-C9 does not fluoresce in organic solvents (e.g., acetonitrile), we found that NP_H could switch between fluorescence (as MC-C9) and nonfluorescence (as SP-C9). UV-irradiation of SP NP_H in aqueous solution created MC NP_H (Figure 1c) with an ~8-fold increase in red fluorescence (600−800 nm) compared to MC-C9 in acetonitrile ([MC-C9] = 0.20 mM for both acetonitrile solution and NP_Hs). The λ_{max} of MC NP_H red-shifted by 32 to 672 nm compared to MC-C9 in acetonitrile (Figure S10a and associated discussion of mechanism). The fluorescence exponential decay constant of MC NP_H (Figure S10b) was 1.44×10^{-4} s^{-1} at 672 nm ($t_{1/2}$ = 4813 s), much slower than for free MC-C9 in acetonitrile solution ($t_{1/2}$ = 346 s). The intensity of the fluorescence and the duration of the decay of that intensity for MC in NP_H would be sufficient for use in microscopic imaging, unlike free MC.

The fluorescent photochromic properties of NPs could be used to track them in biological studies (e.g., intracellular drug delivery) with greater reliability than with simple fluorescence, which can be confounded by interfering fluorophores or in vivo autofluorescence.[46c,47] In fact, NPs surface-modified with SP have been utilized as light-triggerable fluorescent probes.[24h] Here, we evaluated whether fluorescence switching of SP NP_H could be achieved in living cells in vitro in a HeLa cell line (Figure 8a). We loaded Cy5 (emission max = 690 nm) into SP NP_H since its emission spectrum would have little overlap with that of MC NP_H (emission max = 672 nm). Cy5-containing SP NP_Hs were incubated with HeLa cells for 2 h in darkness then exposed to UV illumination for 2 s, causing immediate fluorescence attributable to MC NP_H (Figure 8b). Fluorescence microscopy (Figure 8) indicated that Cy5 (red color) and MC-containing hybrid NPs (green color) were colocalized in HeLa cells (orange color in Figure 8d).

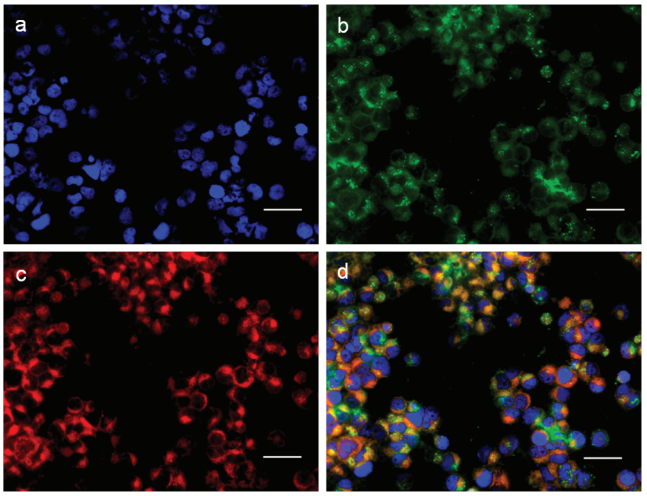

Figure 8. Fluorescence images of the internalization of Cy5-containing NP_H by HeLa cells after 2 h incubation. (a) Nuclear staining with DAPI (blue color). (b) NP_Hs were illuminated by UV for 2s then imaged with 560 nm emission filters (green color); NP_Hs were seen to be internalized. (c) The red color (emission at 700 nm) shows the Cy5 loaded in the SP NP_H. (d) The overlay of panels a−c. The orange color demonstrated colocalization of SP NP_H with Cy5. The scale bar = 50 μm.

Mechanism of Photoswitching NPs. We propose the following assembly model to explain the photoswitching of SP NP_H (Figure 9). The SP NP_Hs are composed of a hydrophilic

dx.doi.org/10.1021/ja211888a | J. Am. Chem. Soc. 2012, 134, 8848−8855

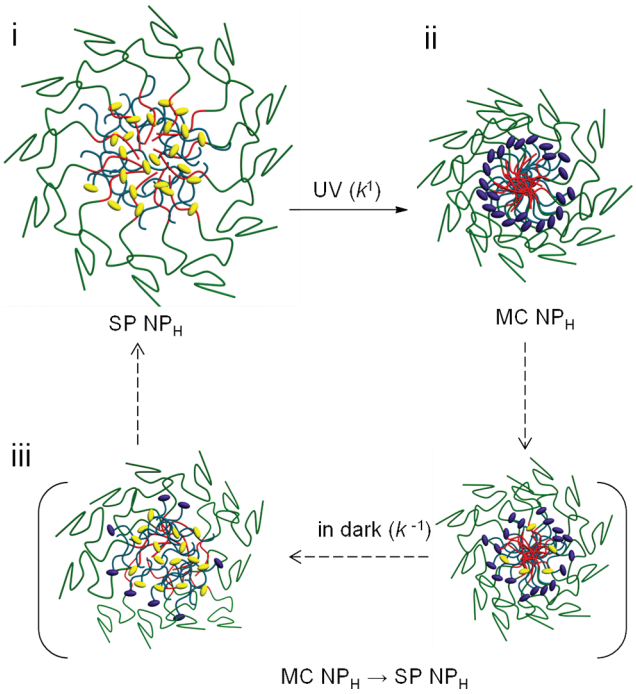

Figure 9. Proposed assembly states of reversible light-triggered SP NP_H size switching: SP NP_H converted MC NP_H upon irradiation (solid arrow, i to ii); graduate transition (dash arrow, ii to iii to i) from MC NP_H to SP NP_H in the dark, with the conversion of zwitterionic MC-C9 to hydrophobic SP-C9 to cause the reassembly of NP_H. Yellow oval, SP molecule; blue line, the alkyl chain in SP; red, lipid part; green line, PEG; and purple oval, MC molecule.

PEG shell, beneath which are the hydrophobic alkyl chains of the DSPE and the SP-C9 (Figure 9i). Given the reported destabilization of monolayer surfactant films by SP,[48] SP is likely to perturb the alkyl chain packing inside the SP NP_H, causing the hydrophobic core to have a loose structure (Figure 9i) and increasing particle size. Upon irradiation, SP converts to zwitterionic MC, that moves outward to relatively polar microenvironments within the NP_H, such as the phosphoglycerol moiety linking DSPE and PEG.[49] The polar microenvironment around MC in NP_H is evidenced by the fact that the λ_{max} of MC in NP_H (551 nm) is comparable to the λ_{max} of MC in polar solvents (Figure S11).[49b] (The effective dielectric constant of the microenvironment of MC in NP_H is ~18, i.e., is relatively polar; detailed discussion in Figure S11.) As MC moves toward the more hydrophilic PEG layer of the NP_H, it moves away from the alkyl chains of the DSPE and lecithin, allowing them to assemble tightly inside the hydrophobic cores; in consequence, the NP_H volume shrinks (Figure 9ii).

The NP_H size will increase again once MC reverts to SP and translocates into the hydrophobic core, perturbing the assembly of the lipids. The alkyl chains of DSPE and lecithin may impede the isomerization of MC to SP, as suggested by the fact that the isomerization in NP_H (λ_{max} = 551 nm) was 12.2-fold slower than that of free MC-C9 in acetonitrile (λ_{max} = 560 nm, Figure S12). This slowing of the isomerization from MC to SP has also been observed in MC in polymeric films.[18a]

CONCLUSION

We have described photoswitchable NP_Hs that allow spatiotemporal controlled release of drugs and enhanced tissue penetration upon UV illumination. This formulation was simple to produce, and tolerated lyophilization, which may facilitate potential clinical translation.[28] The NP_Hs could achieve high loadings with various drugs (chemotherapeutic, local anesthetics). The NP_Hs developed here could be adapted for a range of applications, as they could be modified with functional ligands. The phototriggering system could also be used to enhance NP_H tissue penetration, which might improve antitumor efficacy, penetration into ocular tissue and across the tympanic membrane. This is quite different from conventional approaches, where external energy sources enhance penetration by disrupting tissues.[50]

The photoswitchability is an attractive feature in that it can allow fine spatiotemporal control of drug release: drug is released at the irradiated site, during irradiation. This approach also obviates the need for developing a specific ligand to the tissue of interest. We have previously developed an analogous approach to the same problem by decorating nanoparticles with nonspecific ligands caged with photosensitive chemical protecting groups; upon irradiation, the caging groups would come off, allowing the nanoparticles to bind.[41b] These two approaches and others[13] could prove synergistic.

ASSOCIATED CONTENT

Supporting Information

Experimental details, characterization of SP NP_Hs, in vitro characterization, ex vivo histology, mechanism study. This material is available free of charge via the Internet at http://pubs.acs.org.

AUTHOR INFORMATION

Corresponding Author

Daniel.Kohane@childrens.harvard.edu

Notes

The authors declare no competing financial interest.

ACKNOWLEDGMENTS

The work was supported by a grant from Sanofi-Aventis, and NIH (R21DC009986).

REFERENCES

(1) (a) Langer, R. *Acc. Chem. Res.* **1993**, *26*, 537. (b) Langer, R.; Folkman, J. *Nature* **1976**, *263*, 797.
(2) (a) Gref, R.; Minamitake, Y.; Peracchia, M. T.; Trubetskoy, V.; Torchilin, V.; Langer, R. *Science* **1994**, *263*, 1600. (b) Langer, R. *Nature* **1998**, *392*, 5.
(3) Kost, J.; Langer, R. *Adv. Drug Delivery Rev.* **2001**, *46*, 125.
(4) Farokhzad, O. C.; Langer, R. *ACS Nano* **2009**, *3*, 16.
(5) Jain, R. K.; Stylianopoulos, T. *Nat. Rev. Clin. Oncol.* **2010**, *7*, 653.
(6) (a) O'Brien, M. E. R.; Wigler, N.; Inbar, M.; Rosso, R.; Grischke, E.; Santoro, A.; Catane, R.; Kieback, D. G.; Tomczak, P.; Ackland, S. P.; Orlandi, F.; Mellars, L.; Alland, L.; Tendler, C. *Ann. Oncol.* **2004**, *15*, 440. (b) Gradishar, W. J.; Tjulandin, S.; Davidson, N.; Shaw, H.; Desai, N.; Bhar, P.; Hawkins, M.; O'Shaughnessy, J. *J. Clin. Oncol.* **2005**, *23*, 7794.
(7) Jiang, W.; Kim, B. Y. S.; Rutka, J. T.; Chan, W. C. W. *Nat. Nanotechnol.* **2008**, *3*, 145.
(8) Perrault, S. D.; Walkey, C.; Jennings, T.; Fischer, H. C.; Chan, W. C. W. *Nano Lett.* **2009**, *9*, 1909.
(9) Jain, R. K. *J. Controlled Release* **1998**, *53*, 49.
(10) (a) McKee, T. D.; Grandi, P.; Mok, W.; Alexandrakis, G.; Insin, N.; Zimmer, J. P.; Bawendi, M. G.; Boucher, Y.; Breakefield, X. O.; Jain, R. K. *Cancer Res.* **2006**, *66*, 2509. (b) Netti, P. A.; Berk, D. A.; Swartz, M. A.; Grodzinsky, A. J.; Jain, R. K. *Cancer Res.* **2000**, *60*, 2497. (c) Yuan, F.; Leunig, M.; Huang, S. K.; Berk, D. A.; Papahadjopoulos,

D.; Jain, R. K. *Cancer Res.* **1994**, *54*, 3352. (d) Campbell, R. B.; Fukumura, D.; Brown, E. B.; Mazzola, L. M.; Izumi, Y.; Jain, R. K.; Torchilin, V. P.; Munn, L. L. *Cancer Res.* **2002**, *62*, 6831.
(11) (a) Primeau, A. J.; Rendon, A.; Hedley, D.; Lilge, L.; Tannock, I. F. *Clin. Cancer Res.* **2005**, *11*, 8782. (b) Ouar, Z.; Bens, M.; Vignes, C.; Paulais, M.; Pringel, C.; Fleury, J.; Cluzeaud, F.; Lacave, R.; Vandewalle, A. *Biochem. J.* **2003**, *370*, 185.
(12) Wong, C.; Stylianopoulos, T.; Cui, J. A.; Martin, J.; Chauhan, V. P.; Jiang, W.; Popovic, Z.; Jain, R. K.; Bawendi, M. G.; Fukumura, D. *Proc. Natl. Acad. Sci. U.S.A.* **2011**, *108*, 2426.
(13) Timko, B. P.; Dvir, T.; Kohane, D. S. *Adv. Mater.* **2010**, *22*, 4925.
(14) Youan, B.-B. C. *Adv. Drug Delivery Rev.* **2010**, *62*, 898.
(15) (a) You, S.; Li, W. *Med. Hypotheses* **2008**, *71*, 141. (b) Jain, R. K. *Nat. Med.* **2001**, *7*, 987.
(16) (a) Netti, P. A.; Baxter, L. T.; Boucher, Y.; Skalak, R.; Jain, R. K. *Cancer Res.* **1995**, *55*, 5451. (b) Netti, P. A.; Hamberg, L. M.; Babich, J. W.; Kierstead, D.; Graham, W.; Hunter, G. J.; Wolf, G. L.; Fischman, A.; Boucher, Y.; Jain, R. K. *Proc. Natl. Acad. Sci. U.S.A.* **1999**, *96*, 3137.
(17) (a) Yuan, F.; Chen, Y.; Dellian, M.; Safabakhsh, N.; Ferrara, N.; Jain, R. K. *Proc. Natl. Acad. Sci. U.S.A.* **1996**, *93*, 14765. (b) Yuan, F.; Dellian, M.; Fukumura, D.; Leunig, M.; Berk, D. A.; Torchilin, V. P.; Jain, R. K. *Cancer Res.* **1995**, *55*, 3752.
(18) (a) Tamai, N.; Miyasaka, H. *Chem. Rev.* **2000**, *100*, 1875. (b) Minkin, V. I. *Chem. Rev.* **2004**, *104*, 2751.
(19) Kawata, S.; Kawata, Y. *Chem. Rev.* **2000**, *100*, 1777.
(20) (a) Berkovic, G.; Krongauz, V.; Weiss, V. *Chem. Rev.* **2000**, *100*, 1741. (b) Vlassiouk, I.; Park, C. D.; Vail, S. A.; Gust, D.; Smirnov, S. *Nano Lett.* **2006**, *6*, 1013.
(21) (a) Feringa, B. L.; Browne, W. R. *Nat. Nanotechnol.* **2008**, *3*, 383. (b) Shao, N.; Jin, J. Y.; Wang, H.; Zheng, J.; Yang, R. H.; Chan, W. H.; Abliz, Z. *J. Am. Chem. Soc.* **2010**, *132*, 725.
(22) Tyer, N. W.; Becker, R. S. *J. Am. Chem. Soc.* **1970**, *92*, 1289.
(23) Heiligmanrim, R.; Hirshberg, Y.; Fischer, E. *J. Phys. Chem.* **1962**, *66*, 2465.
(24) (a) Matsumoto, M.; Nakazawa, T.; Mallia, V. A.; Tamaoki, N.; Azumi, R.; Sakai, H.; Abe, M. *J. Am. Chem. Soc.* **2004**, *126*, 1006. (b) Davis, D. A.; Hamilton, A.; Yang, J. L.; Cremar, L. D.; Van Gough, D.; Potisek, S. L.; Ong, M. T.; Braun, P. V.; Martinez, T. J.; White, S. R.; Moore, J. S.; Sottos, N. R. *Nature* **2009**, *459*, 68. (c) Cabrera, I.; Shvartsman, F.; Veinberg, O.; Krongauz, V. *Science* **1984**, *226*, 341. (d) Willner, I. *Acc. Chem. Res.* **1997**, *30*, 347. (e) Lee, H. I.; Wu, W.; Oh, J. K.; Mueller, L.; Sherwood, G.; Peteanu, L.; Kowalewski, T.; Matyjaszewski, K. *Angew. Chem., Int. Ed.* **2007**, *46*, 2453. (f) Osborne, E. A.; Jarrett, B. R.; Tu, C. Q.; Louie, A. Y. *J. Am. Chem. Soc.* **2010**, *132*, 5934. (g) Zhu, M. Q.; Zhu, L. Y.; Han, J. J.; Wu, W. W.; Hurst, J. K.; Li, A. D. Q. *J. Am. Chem. Soc.* **2006**, *128*, 4303. (h) Zhu, L. Y.; Zhu, M. Q.; Hurst, J. K.; Li, A. D. Q. *J. Am. Chem. Soc.* **2005**, *127*, 8968.
(25) Movia, D.; Prina-Mello, A.; Volkov, Y.; Giordani, S. *Chem. Res. Toxicol.* **2010**, *23*, 1459.
(26) Cheng, J.; Teply, B. A.; Sherifi, I.; Sung, J.; Luther, G.; Gu, F. X.; Levy-Nissenbaum, E.; Radovic-Moreno, A. F.; Langer, R.; Farokhzad, O. C. *Biomaterials* **2007**, *28*, 869.
(27) Kjoniksen, A. L.; Joabsson, F.; Thuresson, K.; Nystrom, B. *J. Phys. Chem. B* **1999**, *103*, 9818.
(28) Tong, R.; Yala, L.; Fan, T. M.; Cheng, J. *Biomaterials* **2010**, *31*, 3043.
(29) Fang, R. H.; Aryal, S.; Hu, C. M. J.; Zhang, L. F. *Langmuir* **2010**, *26*, 16958.
(30) Malatesta, V.; Neri, C.; Wis, M. L.; Montanari, L.; Millini, R. *J. Am. Chem. Soc.* **1997**, *119*, 3451.
(31) Klibanov, A. L.; Maruyama, K.; Torchilin, V. P.; Huang, L. *FEBS Lett.* **1990**, *268*, 235.
(32) Popielarski, S. R.; Pun, S. H.; Davis, M. E. *Bioconjugate Chem.* **2005**, *16*, 1063.
(33) Abdelwahed, W.; Degobert, G.; Stainmesse, S.; Fessi, H. *Adv. Drug Delivery Rev.* **2006**, *58*, 1688.
(34) Tong, R.; Yala, L. D.; Fan, T. M.; Cheng, J. J. *Biomaterials* **2010**, *31*, 3043.
(35) Mosmann, T. *J. Immunol. Methods* **1983**, *65*, 55.
(36) Draft Guidance on Doxorubicin Hydrochloride. http://www.fda.gov/downloads/Drugs/GuidanceComplianceRegulatoryInformation/Guidances/UCM199635.pdf.
(37) Baillet, G.; Giusti, G.; Guglielmetti, R. *J. Photochem. Photobiol., A* **1993**, *70*, 157.
(38) Patel, H.; Tscheka, C.; Heerklotz, H. *Soft Matter* **2009**, *5*, 2849.
(39) (a) Petros, R. A.; DeSimone, J. M. *Nat. Rev. Drug Discovery* **2010**, *9*, 615. (b) Davis, M. E.; Chen, Z.; Shin, D. M. *Nat. Rev. Drug Discovery* **2008**, *7*, 771.
(40) (a) Farokhzad, O. C.; Cheng, J. J.; Teply, B. A.; Sherifi, I.; Jon, S.; Kantoff, P. W.; Richie, J. P.; Langer, R. *Proc. Natl. Acad. Sci. U.S.A.* **2006**, *103*, 6315. (b) Cao, Z. H.; Tong, R.; Mishra, A.; Xu, W. C.; Wong, G. C. L.; Cheng, J. J.; Lu, Y. *Angew. Chem., Int. Ed.* **2009**, *48*, 6494.
(41) (a) Chan, J. M.; Zhang, L. F.; Tong, R.; Ghosh, D.; Gao, W. W.; Liao, G.; Yuet, K. P.; Gray, D.; Rhee, J. W.; Cheng, J. J.; Golomb, G.; Libby, P.; Langer, R.; Farokhzad, O. C. *Proc. Natl. Acad. Sci. U.S.A.* **2010**, *107*, 2213. (b) Dvir, T.; Banghart, M. R.; Timko, B. P.; Langer, R.; Kohane, D. S. *Nano Lett.* **2010**, *10*, 250.
(42) Ramanujan, S.; Pluen, A.; McKee, T. D.; Brown, E. B.; Boucher, Y.; Jain, R. K. *Biophys. J.* **2002**, *83*, 1650.
(43) Sionkowska, A.; Wess, T. *Int. J. Biol. Macromol.* **2004**, *34*, 9.
(44) Vinegoni, C.; Botnaru, I.; Aikawa, E.; Calfon, M. A.; Iwamoto, Y.; Folco, E. J.; Ntziachristos, V.; Weissleder, R.; Libby, P.; Jaffer, F. A. *Sci. Transl. Med.* **2011**, *3*, 84ra45.
(45) Cabral, H.; Matsumoto, Y.; Mizuno, K.; Chen, Q.; Murakami, M.; Kimura, M.; Terada, Y.; Kano, M. R.; Miyazono, K.; Uesaka, M.; Nishiyama, N.; Kataoka, K. *Nat. Nanotechnol.* **2011**, *6*, 815.
(46) (a) Marriott, G.; Mao, S.; Sakata, T.; Ran, J.; Jackson, D. K.; Petchprayoon, C.; Gomez, T. J.; Warp, E.; Tulyathan, O.; Aaron, H. L.; Isacoff, E. Y.; Yan, Y. L. *Proc. Natl. Acad. Sci. U.S.A.* **2008**, *105*, 17789. (b) Zhu, M. Q.; Zhang, G. F.; Li, C.; Aldred, M. P.; Chang, E.; Drezek, R. A.; Li, A. D. Q. *J. Am. Chem. Soc.* **2011**, *133*, 365. (c) Ntziachristos, V.; Ripoll, J.; Wang, L. V.; Weissleder, R. *Nat. Biotechnol.* **2005**, *23*, 313. (d) Srinivasan, S.; Pogue, B. W.; Jiang, S.; Dehghani, H.; Kogel, C.; Soho, S.; Gibson, J. J.; Tosteson, T. D.; Poplack, S. P.; Paulsen, K. D. *Proc. Natl. Acad. Sci. U.S.A.* **2003**, *100*, 12349. (e) Yoder, E. J.; Kleinfeld, D. *Microsc. Res. Tech.* **2002**, *56*, 304.
(47) Zhu, L. Y.; Wu, W. W.; Zhu, M. Q.; Han, J. J.; Hurst, J. K.; Li, A. D. Q. *J. Am. Chem. Soc.* **2007**, *129*, 3524.
(48) (a) Khairutdinov, R. F.; Hurst, J. K. *Langmuir* **2001**, *17*, 6881. (b) Holden, D. A.; Ringsdorf, H.; Deblauwe, V.; Smets, G. *J. Phys. Chem.* **1984**, *88*, 716. (c) Gruler, H.; Vilanove, R.; Rondelez, F. *Phys. Rev. Lett.* **1980**, *44*, 590.
(49) (a) Mazeres, S.; Schram, V.; Tocanne, J. F.; Lopez, A. *Biophys. J.* **1996**, *71*, 327. (b) Khairutdinov, R. F.; Giertz, K.; Hurst, J. K.; Voloshina, E. N.; Voloshin, N. A.; Minkin, V. I. *J. Am. Chem. Soc.* **1998**, *120*, 12707.
(50) (a) Hu, M.; Chen, J. Y.; Li, Z. Y.; Au, L.; Hartland, G. V.; Li, X. D.; Marquez, M.; Xia, Y. N. *Chem. Soc. Rev.* **2006**, *35*, 1084. (b) Kong, G.; Braun, R. D.; Dewhirst, M. W. *Cancer Res.* **2000**, *60*, 4440. (c) Jain, P. K.; Lee, K. S.; El-Sayed, I. H.; El-Sayed, M. A. *J. Phys. Chem. B* **2006**, *110*, 7238.